

# Investigation of metrics for readout-independent evaluation of the functional robustness of liquid state machines

Naoki Hirata<sup>†</sup> and Naoki Wakamiya<sup>†</sup>

<sup>†</sup>Graduate School of Information Science and Technology, Osaka University  
1-5 Yamadaoka, Suita, Osaka 565-0871, Japan  
Email: {n-hirata, wakamiya}@ist.osaka-u.ac.jp

**Abstract**—Physical reservoir computing, which is the physical implementation of reservoir computing models, has attracted attention of researchers. Although it has a variety of applications, as a physical entity, it is prone to physical failures. Therefore, it is necessary to design a reservoir which is functionally robust to failures. More specifically, it is desired that a reservoir maintains the dynamics even after failures. For this purpose, in this paper, we investigate metrics to evaluate the functional robustness of a reservoir. By comparing distance metrics, we found that D-spike and D-interval were suitable for such evaluation.

## 1. Introduction

The reservoir computing is a type of computational models based on neural networks [1]. It consists of three layers: an input layer, an intermediate layer called a reservoir, and an output layer. The input is projected to the dynamics of the internal state of a high-dimensional and nonlinear reservoir, which is then read out and transformed to the desired output. Unlike general machine learning methods using neural networks, the structure and weights of connections of a reservoir can be fully random. Furthermore, only weights of connections from the reservoir to the output layer are adjusted during training. Due to its simplicity and the universal approximation property, research on physical reservoir computing, in which reservoirs are implemented in physical systems such as semiconductor lasers and soft materials, has been actively conducted [1].

Previous studies have verified the performance of physical reservoir computing, but they assumed the stability of the reservoir. However, as a physical entity, physical failures are very likely to occur and the structure of the reservoir changes. As a result, the dynamics of the reservoir changes and thus readout fails. Thus performance degradation is not avoidable. Although training during operation sometimes is possible, it is not guaranteed that the performance is fully recovered.

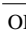

To tackle the problem, in [2], they investigated the reservoir structure which was robust to physical failures. Since their focus was on the robustness to maintain the performance not the structural properties, it was called the func-

tional robustness. They used a liquid state machine (LSM), which is a type of reservoir computing model explaining information processing in the neocortex of the human brain, and evaluated the relationship between the structure of a reservoir, called a liquid, and the degree of degradation in performance of a delayed readout task when facing to loss of neurons and disconnection of synaptic connections. The results showed that the high modularity, irregularity, and high clustering coefficient contributed to the functional robustness. However, the task performance depends not only on the reservoir structure but a readout algorithm. Therefore, it is necessary to train and test a reservoir to design a physically robust reservoir.

The performance of an LSM depends on two properties called the separation property and the approximation property. The former is related to a liquid, meaning the capability of generating diverse and input-dependent dynamics. The latter is related to readout, that is, the capability of mapping the dynamics of a liquid to a desired input-dependent output. It implies that the functional robustness can be assessed based purely on the structure of a liquid without using a specific task.

Therefore, in this paper, we investigated metrics to evaluate the functional robustness of a liquid from a viewpoint of the dynamics of the liquid and identified those well expressing the performance degradation caused by physical failures. The liquid dynamics is in the form of a time series of spikes that neurons emit for given inputs. Therefore, we assumed that the magnitude of the change in spike trains was correlated with the magnitude of the decrease in the performance of an LSM. We compared the change in distances of four distance metrics and additional one metric from a viewpoint of correlation with the change in the task performance, while disconnecting synaptic connections at random, using six network models. We used the NARMA (nonlinear autoregressive moving average) [3] task, that is, a benchmark task of reservoir computing, as the first step of our research. In the following we call a neuron and a synaptic connection as a node and a link, respectively.

The remainder of the paper is organized as follows. First in section 2, we introduce metrics we used in the evaluation. Next section 3 summarizes network models to generate liquids with a variety of structural properties. Then in section 4, the setting in the evaluation is described. Section

ORCID iDs Naoki Hirata:  0000-0002-8534-1642, Naoki Wakamiya:  0000-0002-6195-6087



This work is licensed under a Creative Commons Attribution NonCommercial, No Derivatives 4.0 License.

5 gives results and discussion. Finally section 6 summarizes the paper and shows future directions.

## 2. Distance metrics

A spike train of node  $i$  is expressed as  $T_i = (t_i(1), t_i(2), \dots, t_i(n_i))$ , where  $t_i(k)$  is the time when  $k$ -th spike was emitted by node  $i$  and  $n$  is the number of spikes of node  $i$ . Given a pair of spike trains  $T_1$  and  $T_2$ , the Hamming distance is derived as  $|T_1| + |T_2| - |\{(k, j) | t_1(k) = t_2(j)\}|$ .

We also evaluated the modulus-metric proposed in [4]. It is based on the Hausdorff distance, which is a function of the distance between an arbitrary time and the nearest spike. The distance is derived as the integral of the difference between two spike trains. Given two spike trains  $T_1$  and  $T_2$ , the modulus-metric  $d$  between them is given by

$$d = \int |d(s, T_1) - d(s, T_2)| ds, \quad (1)$$

where  $d(s, T) = \inf_{t \in T} |t - s|$  for time  $s \in \mathbb{R}$ . If either of spike trains contains no spike at all,  $d(s, T)$  cannot be defined. Thus the distance is considered zero [4].

Additionally, we used the D-spike and D-interval. The D-spike quantifies the cost of adding, removing, and moving spikes to match two spike trains [5]. The cost of addition and removal of a spike is one. The cost of moving a spike by time  $\Delta t$  is given as  $q\Delta t$ .  $q$  ( $q \geq 0$ ) is a parameter. The minimum cost of manipulation is regarded as the distance. The case of  $q = 0$  is called the D-count, where the difference in the number of spikes is the distance. The D-interval quantifies the cost of adding, removing, extending, and shortening spike intervals [5]. The cost of addition and removal of an interval is one and the cost of extension and shortening is  $q\Delta t$ . The minimum cost is the distance. We considered 1 [ms] as the moving distance  $\Delta t = 1$ .

In addition to those spike train metrics, we evaluated the spectral radius, which is used as an indicator of the performance of an echo state network, that is, another reservoir computing model [6]. The spectral radius is derived as the maximum absolute value of eigenvalues of an adjacency matrix of a neural network. We defined the difference in the spectral radii before and after physical failures as the distance.

## 3. Network model

To investigate the influence of the liquid structure on distance metrics and task performance in facing to physical failures, we used six network models: random (RD), Watts-Strogatz (WS), ring (RI), Barabási-Albert (BA), distance-based (DB), and human connectome (HC). The RD connected a pair of randomly selected nodes by a link in the random direction, without allowing duplicated connections, until the number of links reached the targeted number. A WS network was generated based on [7], where the rewiring probability was 0.2. A network before rewiring

was called a RI network. Regarding the BA [8], the size of an initial network was 5.

With the DB, a link was established between a pair of nodes in a stochastic manner. Specifically, the probability to connect node  $a$  to node  $b$  was given as  $C \exp\left(-\left(\frac{D(a,b)}{\lambda}\right)^2\right)$ , where  $D(a, b)$  is their Euclidean distance. The parameter  $C$  was 0.3, 0.2, 0.4, or 0.1, depending on the type of nodes, i.e., excitatory (E) or inhibitory (I), as EE, EI, IE, and II, respectively.  $\lambda$  was set at 1.5.

Finally, the HC [9] generated a network which had the degree distribution, the clustering coefficient, the betweenness centrality, and the edge length distribution similar to the human connectome. It was accomplished by connecting nodes  $a$  and  $b$  with the probability  $D(a, b)^\eta K(a, b)^\gamma$ , where  $K(a, b) = \frac{|\Gamma_{a \setminus b} \cap \Gamma_{b \setminus a}|}{|\Gamma_{a \setminus b} \cup \Gamma_{b \setminus a}|}$ . Here,  $\Gamma_{a \setminus b}$  is a set of nodes connected with node  $a$  except for node  $b$ .

## 4. Setting

In the NARMA task, the input  $u(n)$  was a series of uniform random numbers in the range of 0 to 0.5. The task was to estimate a series of  $d(n)$  defined as follows.

$$d(n+1) = a_1 d(n) + a_2 d(n) \sum_{i=0}^{m-1} \{d(n-i) + a_3 u(n-m+1)u(n) + a_4\} \quad (2)$$

The parameter  $m$  corresponds to the number of preceding steps which the output  $d(n)$  depends on. Therefore, it is necessary for a liquid to have the sufficient memory capacity to accurately estimate  $d(n)$  with a large  $m$ .

In our evaluation, each  $u(n)$  was given to 30% of nodes in a liquid as a constant input for the period of 1.5 [ms]. We used  $a_1 = 0.3$ ,  $a_2 = 0.05$ ,  $a_3 = 1.5$ , and  $a_4 = 0.1$ . Then, based on spike trains of all nodes during the period, an output layer estimated  $d(n)$  by using the Ridge regression.

We first generated 100 liquid networks of 200 nodes for each of the network models. Next, for each network, we evaluated the task performance of the cases of 10 different values of  $m = 2, 4, 6, \dots, 20$  and 10 different setting of link failures: no failure, 10%, 20%,  $\dots$ , 90% of links were randomly removed from a liquid. As a performance measure, we used the normalized root mean square error (NRMSE). For each of failure probability, NRMSE was averaged over results of 10 values of  $m$  of each network of each network model. Finally, by subtracting the average NRMSE without failures from the average NRMSE with failures, we obtained the change in NRMSE for each network of each network model. Regarding the distance metrics, first the distance was calculated between spike trains before and after failures of a certain failure probability for each of 200 nodes of each network of each network model. Then, the distance was averaged over 200 nodes and we obtained the change in the distance for each network of each network

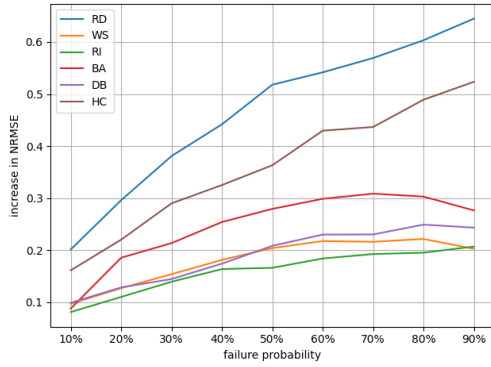


Figure 1: Relationship between failure probability and estimation error

model. Finally, we evaluated the correlation coefficient between a pair of the change in NRMSE and the change in the distance for each network of each network model.

## 5. Results

Figure 1 shows the changes in the average estimation error. As shown in Fig. 1, the estimation error monotonically increased as the failure probability increased, independently of network models. On the contrary, depending on metrics, there are a variety of curves in Fig. 2 for the case of the RD as an example. The correlation coefficients are summarized in Fig. 3 using violin plots. Red dots represent averages. Upper and lower horizontal bars show the maximum and minimum coefficients, respectively. Although all metrics had the wide distribution and there were differences among network models, the D-spike except for  $q = 1$  and D-interval had the relatively high correlation.

The spectral radius had the high correlation in the RD and HC. Basically, from its definition, the spectral radius is related to the number of elements in an adjacency matrix. As a result, the distance linearly increased as the number of links decreased. On the other hand, Fig. 1 shows that the increase in the change in the estimation error became small when the failure probability was high in the WS, RI, BA, and DB models, which resulted in the low correlation.

Regarding the Hamming distance, the correlation was relatively low and similar with the D-spike ( $q = 1$ ). Since spike emission was intermittent and sparse, the Hamming distance was well related to the number of spikes. Actually, the correlation coefficient between the Hamming distance and the change in the number of spiked before and after failures was 0.999. In the range of small failure probability, the number of spikes increased, because removing links from inhibitory nodes had the strong influence to allow nearby nodes to emit spikes. On the other hand, in the range of high failure probability, where many links had already been removed, the number of spikes decreased. It is a reason why the Hamming distance had the peak at

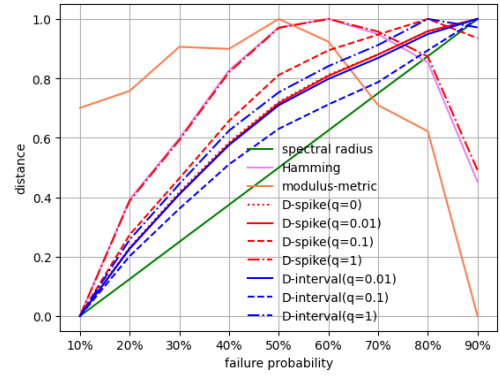


Figure 2: Relationship between failure probability and distance (RD model)

the failure probability of 60% and the correlation became small. In the case of the D-spike ( $q = 1$ ), because moving a spike costs much, addition and removal of spikes were mainly conducted. Therefore, the distance corresponded to the number of spikes similarly with the Hamming distance.

The modulus-metric had the lowest correlation coefficient. Based on the definition, the average of  $d(s, T)$  decreases as the number of spikes increases, and vice versa. Therefore, the difference between averages of  $d(s, T_1)$  and  $d(s, T_2)$  increased as the difference in the number of spikes in spike trains  $T_1$  and  $T_2$  increased. As discussed, the number of spikes first decreases and then increases according to the failure probability. In addition, there were nodes that did not emit spikes at all. In such a case, the distance was considered zero, which affected the distance. Consequently the change in the distance had the peak at the failure probability of 50%, and it made the correlation coefficient low.

The correlation coefficients of D-spike except for  $q = 1$  and D-interval were high in the RD and HC models. These distances were roughly proportional to the absolute value of the difference in the number of spikes, whereas the value of  $q$  affected the results. As discussed, the average difference in the number of spikes had the peak at the failure probability of around 60%. However, unlike the Hamming distance, those metrics kept increasing. As mentioned in the case of the modulus-metric, there were nodes that did not fire at all due to failures. On such nodes, the difference in the number of spikes before and after failures became negative and rapidly decreased. As a result, the absolute value of the difference kept increasing and thus the distance of those metrics monotonically increased. Consequently, the change in the distance had the high correlation with the change in the estimation error of the RD and HC models.

## 6. Conclusion

In this paper, we investigated distance metrics to evaluate the functional robustness of a liquid from its dynamics. As a result, we found that D-spike ( $q = 0, 0.01, \text{ and } 0.1$ )

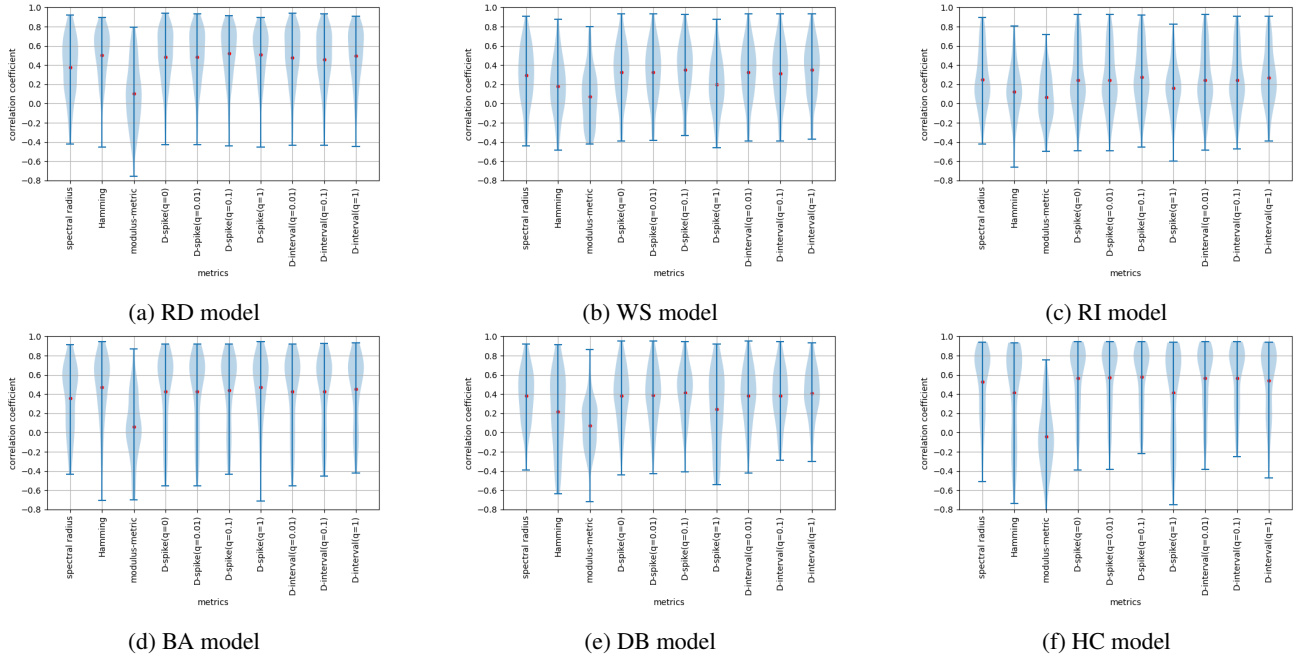


Figure 3: Correlation coefficient between distance metrics and estimation error

and D-interval ( $q = 0, 0.01, 0.1$ , and  $1$ ) were suitable for evaluation especially for the RD and HC model networks.

However, those metrics had lower correlation for the other models. Therefore, as the next step of the research, we plan to investigate and design distance metrics which are highly correlated with the performance independently of network models. In parallel to this, we also need to examine other tasks to confirm task and readout-independent distance metrics. Furthermore, we need to consider node failures, where not only a node but all connected links are lost at once. It affects both of the dynamics of a liquid and the performance.

## Acknowledgments

This work was partly supported by JSPS KAKENHI Grant Number JP21K11867 and JP21H03515.

## References

- [1] G. Tanaka, T. Yamane, J. B. Héroux, R. Nakane, N. Kanazawa, S. Takeda, H. Numata, D. Nakano, and A. Hirose, “Recent advances in physical reservoir computing: A review,” *Neural Networks*, vol. 115, pp. 100–123, Mar. 2019.
- [2] Y. Okumura and N. Wakamiya, “Analysis of reservoir structure contributing to robustness against structural failure of liquid state machine,” *ICANN Artificial Neural Networks and Machine Learning*, pp. 435–446, Oct. 2020.
- [3] A. Atiya and A. Parlos, “New results on recurrent network training: unifying the algorithms and accelerating convergence,” *IEEE Transactions on Neural Networks*, vol. 11, pp. 697–709, May 2000.
- [4] C. V. Rusu and R. V. Florian, “A new class of metrics for spike trains,” *Neural Computation*, vol. 26, p. 306–348, Feb. 2014.
- [5] J. D. Victor and K. P. Purpura, “Metric-space analysis of spike trains: theory, algorithms and application,” *Network: Computation in Neural Systems*, vol. 8, pp. 127–164, Jan. 1997.
- [6] J. Jiang and Y.-C. Lai, “Model-free prediction of spatiotemporal dynamical systems with recurrent neural networks: Role of network spectral radius,” *Phys. Rev. Research*, vol. 1, p. 033056, Oct 2019.
- [7] D. J. Watts and S. H. Strogatz, “Collective dynamics of ‘small-world’ networks,” *Nature*, vol. 393, pp. 440–442, June 1998.
- [8] R. Albert and A.-L. Barabási, “Statistical mechanics of complex networks,” *Reviews of Modern Physics*, vol. 74, p. 47–97, Jan. 2002.
- [9] R. F. Betzel, A. Avena-Koenigsberger, J. Goñi, Y. He, M. A. de Reus, A. Griffa, P. E. Vértes, B. Mišić, J.-P. Thiran, P. Hagmann, M. van den Heuvel, X.-N. Zuo, E. T. Bullmore, and O. Sporns, “Generative models of the human connectome,” *NeuroImage*, vol. 124, pp. 1054–1064, Jan. 2016. 26427642[pmid].